

## Controlling wettability of PECVD-deposited dual organosilicon/carboxylic acid films to influence DNA hybridisation assay efficiency

*S.P. Flynn<sup>1,2\*</sup>, R. Monaghan<sup>1,3</sup>, J. Bogan<sup>4</sup>, M. McKenna<sup>1,3</sup>, A Cowley<sup>1</sup>, S Daniels<sup>1,4</sup>, G. Hughes<sup>3</sup> and S M Kelleher<sup>1,2\*</sup>*

<sup>1</sup> National Centre for Plasma Science and Technology, Glasnevin, Dublin 9, Ireland

<sup>2</sup> School of Chemistry, University College Dublin, Belfield, Dublin 4, Ireland

<sup>3</sup> Biomedical Diagnostic Institute, Dublin City University, Dublin 9, Ireland

<sup>4</sup> School of Physical Sciences, Dublin City University, Dublin 9, Ireland

\*Corresponding authors: Tel +35317162839, E-mail: [susan.kelleher@ucd.ie](mailto:susan.kelleher@ucd.ie)

Tel +35317006337, E-mail: [shauna.flynn2@mail.dcu.ie](mailto:shauna.flynn2@mail.dcu.ie)

### Supplementary Information

List of contents

**Figure S1** – PECVD instrumentation

**Figure S2** – Thickness changes after washing of plasma-deposited TEOS and AA

**Figure S3** – AFM images of hydrophilic and hydrophobic TEOS/AA

**Figure S4** – XRR fit data

**Figure S5** – FTIR results

**Figure S6** – XPS survey spectra highlighting the change in chemical composition between hydrophobic and hydrophilic TEOS/AA samples

**Table S1** – Concentrations of Silicon, carbon and oxygen in each sample according to the XPS survey spectra.

**Figure S7** – Fluorescent images showing binding with and without EDC

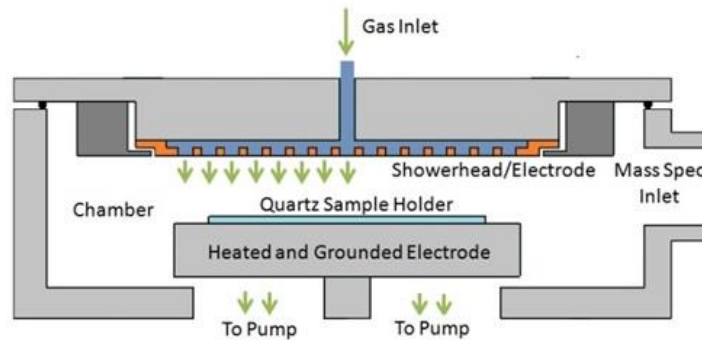


**Figure S1.** Cross section schematic of Oxford Instruments Plasmalab System100 PECVD reactor showing the dispersal showerhead and sample positioning.

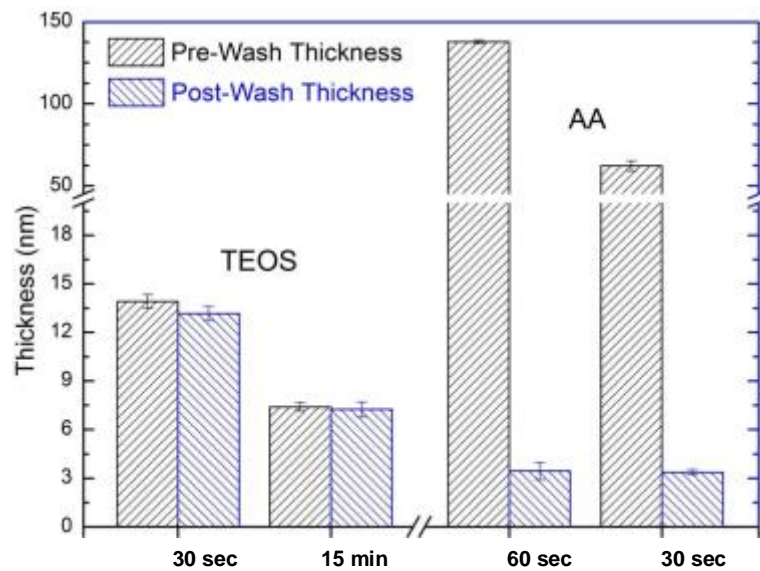


**Figure S2 .** (Left) TEOS thickness stability over multiple processes and post wash thickness and (Right) AA process stability over multiple runs and subsequent changes due to washing. Deposition times for TEOS were 30 and 15 sec; deposition times for AA were 60 and 30 sec.

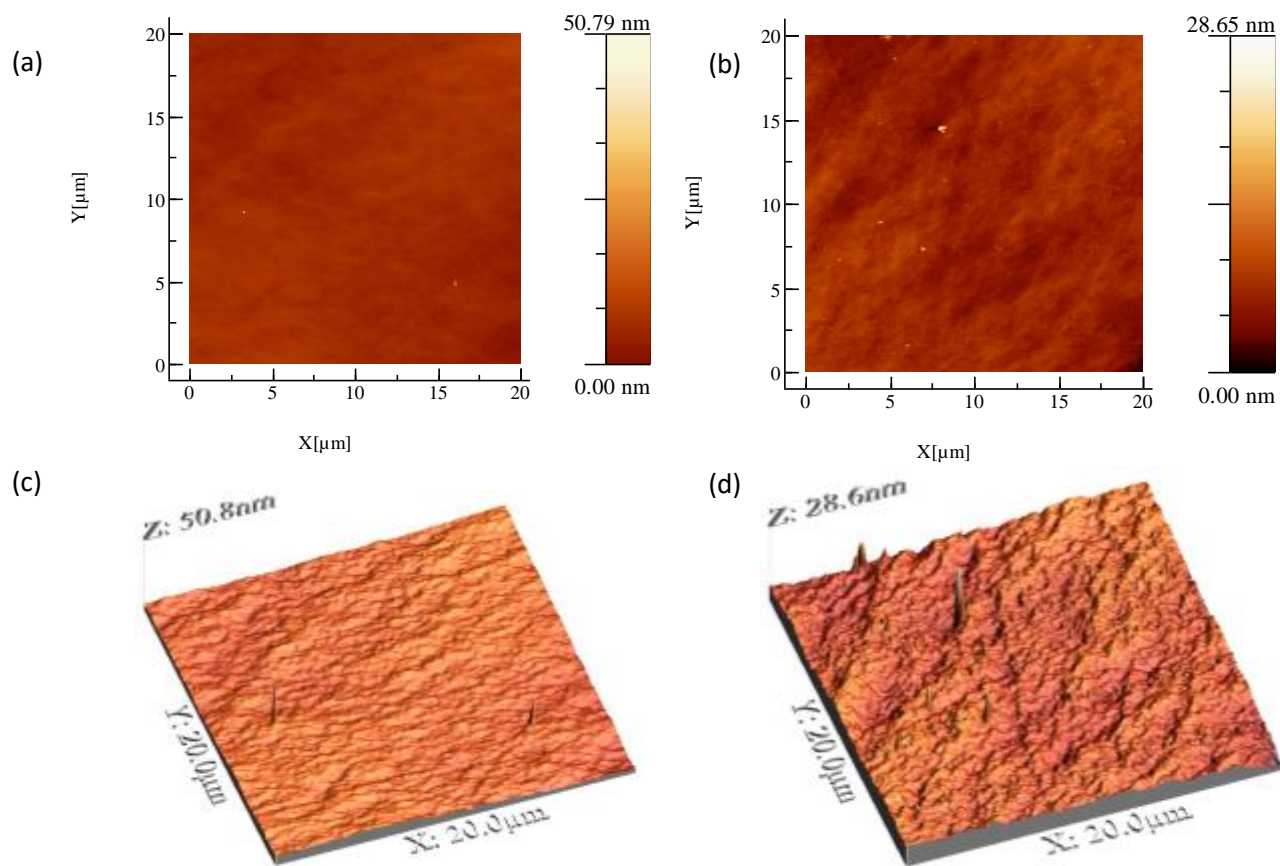


**Figure S3.** AFM images of hydrophobic TEOS/AA (a) and (c). AFM images of hydrophilic TEOS/AA (b) and (d).

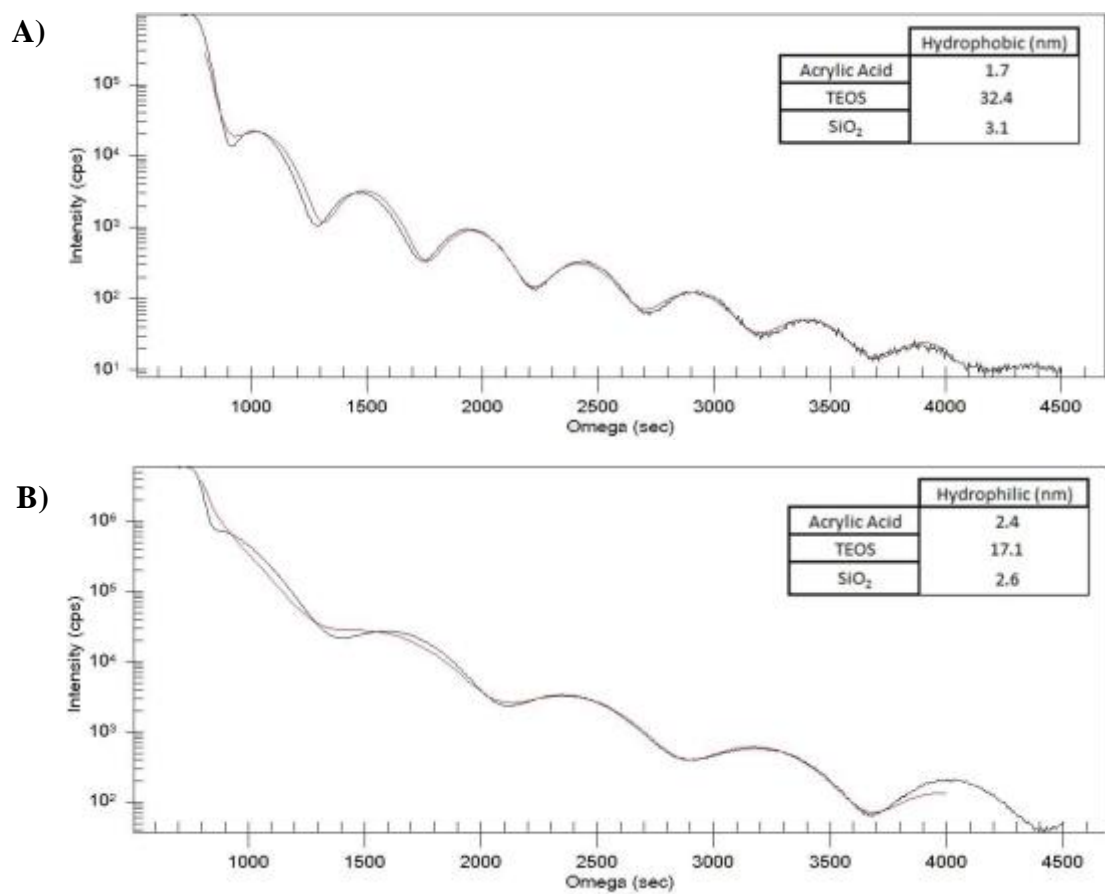


**Figure S4.** XRR data fits for **a)** hydrophobic TEOS/AA and **b)** hydrophilic TEOS/AA

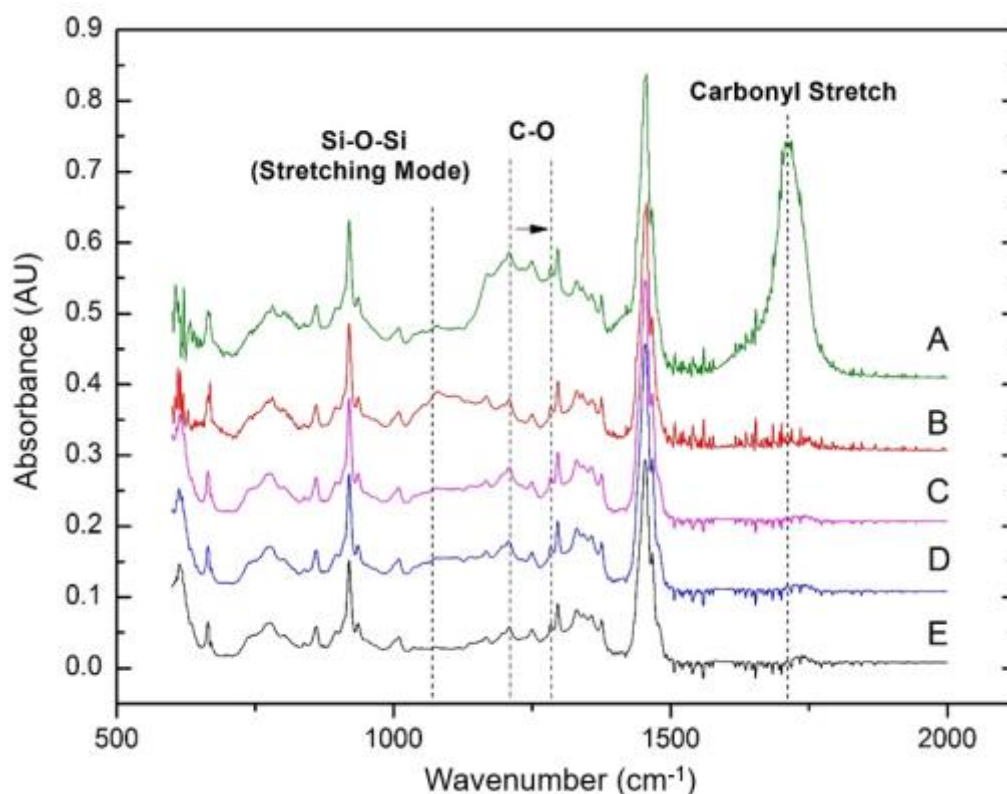


**Figure S5.** Shows the elemental similarities and differences between as-deposited TEOS/AA (A), plain TEOS (B), TEOS/AA<sub>10</sub> (C), TEOS/AA<sub>75</sub> (D) and plain Zeonor (E) samples using FTIR

Sample A shows a distinct peak present around  $1700\text{ cm}^{-1}$ , an area relating to carbonyl stretching mode. This is bolstered by an increased peak intensity around  $1200\text{-}1280\text{ cm}^{-1}$ , relating to C-O bonding, collectively displaying a large presence of carboxyl groups in the wbAA polymer layer. When washed away, for both the hydrophilic and hydrophobic TEOS/AA samples (C and D respectively), these peaks are immeasurable. These match the profile of the plain Zeonor in sample E, showing the cbAA layer to be extremely thin and immeasurable on the FTIR system. The only mildly discernible peaks present on samples C and D are at  $1071\text{ cm}^{-1}$ , which relates to Si-O-Si stretching mode, indicating the present of a silicon-based film, although the signal strength matches the relative thinness of the film. This peak matches that found on both the A sample data, and the peak is more prominent on sample B, proving that it relates directly to the silicon bottom layer. Although a faint increase is observed at the peaks relating to Si-O-Si stretching modes, it is concluded that the cbAA layer is too thin for accurate examination using FTIR.

**Table S1.** Concentrations of Silicon, carbon and oxygen in each sample according to the survey spectra.

Sample	Silicon (%)	Carbon (%)	Oxygen (%)
<b>(a) TEOS Reference</b>	32	29	39
<b>(b) Hydrophobic TEOS/AA<sub>75</sub></b>	28	30	42
<b>(c) Hydrophilic TEOS/AA<sub>10</sub></b>	39	15	46

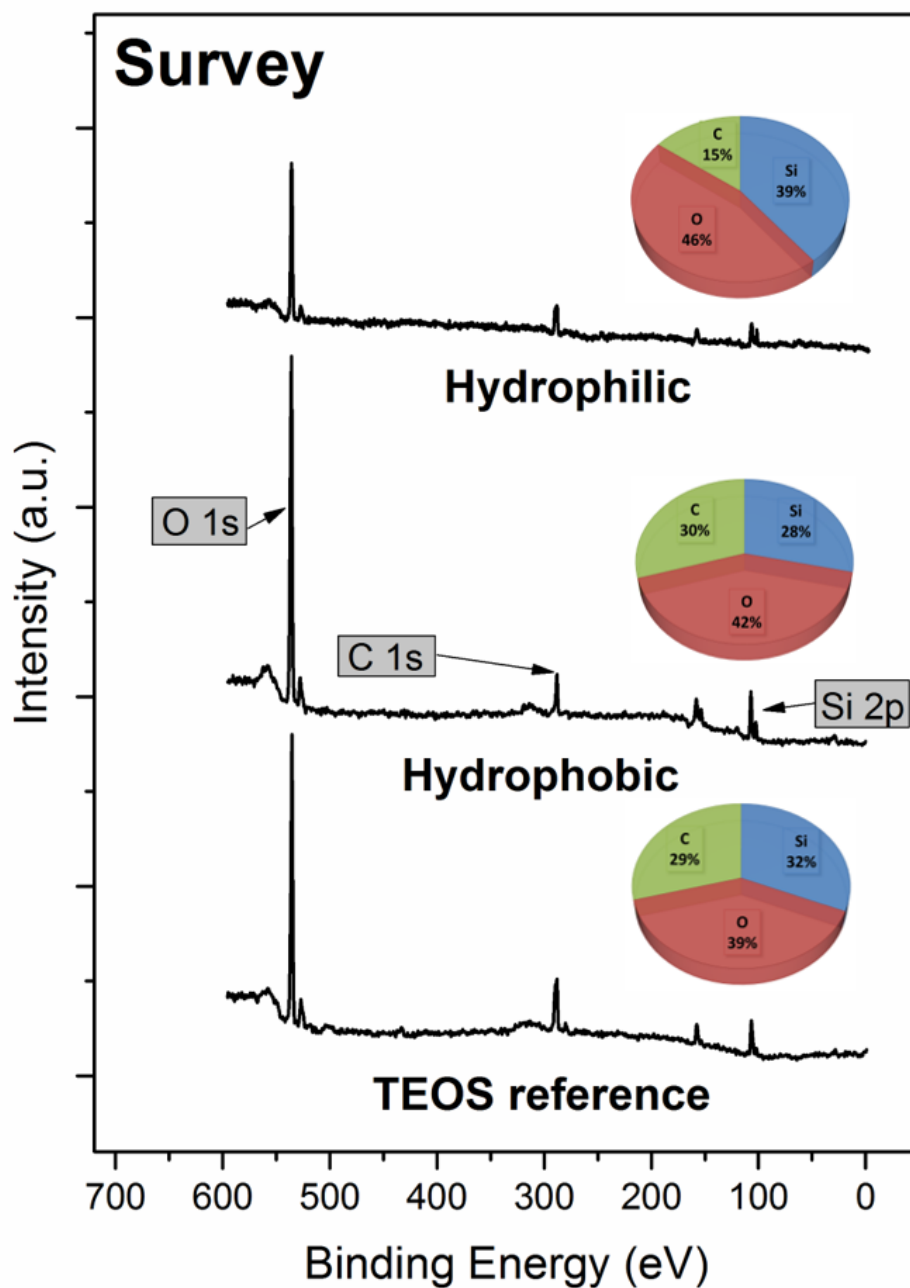


**Figure S6.** XPS survey spectra highlighting the change in chemical composition between hydrophobic and hydrophilic TEOS/AA samples

The survey spectra of the TEOS reference film (a) contains Si 2p, Si 2s, and O 1s transitions consistent with RF plasma deposited TEOS film. A significant C 1s peak is observed as the TEOS film is not subject to the hydrolysis reaction which commonly converts it to  $\text{SiO}_2^1$ . This is relevant as narrow energy window C 1s spectra are routinely/commonly used for the

identification of acrylic acid using XPS<sup>2</sup>, and the additional carbon peaks inherent to TEOS will complicate chemical analysis. Identification of the AA using the O 1s spectra will also be complicated by the presence of a large oxygen signal again from the TEOS underlayer.

The hydrophobic dual layer TEOS/AA<sub>75</sub> deposited film (b) shows minimal change in chemical composition compared with the reference TEOS. This indicates that only trace amounts of AA are detectable within the XPS survey spectra. Conversely, the hydrophilic dual layer TEOS/AA<sub>10</sub> (c) shows a significant change in chemical composition with the apparent decrease of carbon suggesting a significant change in chemistry at the TEOS/AA interface.

**Figure S7** shows a representative image of the fluorescent intensity of the labelled DNA with and without EDC at different concentrations (10  $\mu$ M and 1  $\mu$ M). This demonstrates the lack of non-specific binding when the TEOS/AA surfaces interact with the DNA probes. Top row has no EDC; bottom row has EDC; two LHS spots have 10  $\mu$ M DNA; two RHS spots have 1  $\mu$ M DNA. Scanned at Gain 90.

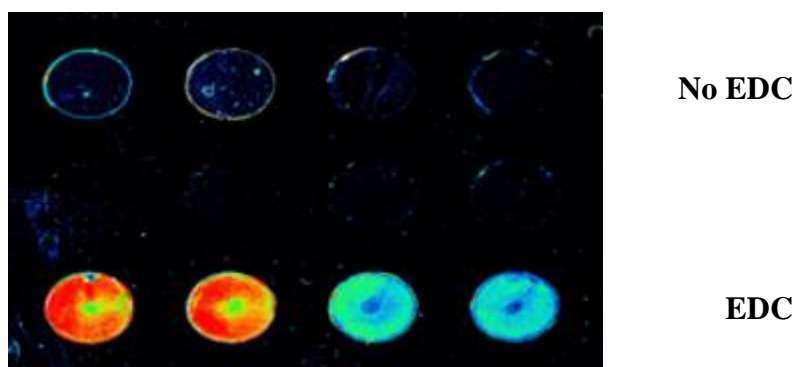


*Figure S7*

## References

1. Bulla DAP, Morimoto NI. Deposition of thick TEOS PECVD silicon oxide layers for integrated optical waveguide applications. *Thin Solid Films*. 1998;334(1):60-64.  
<http://www.sciencedirect.com/science/article/pii/S0040609098011171>. Accessed Jun 27, 2017. doi: 10.1016/S0040-6090(98)01117-1.
2. Leadley SR, Watts JF. The use of XPS to examine the interaction of poly(acrylic acid) with oxidised metal substrates. *Journal of Electron Spectroscopy and Related Phenomena*. 1997;85(1):107-121. <http://www.sciencedirect.com/science/article/pii/S0368204897000285>. Accessed Jun 27, 2017. doi: 10.1016/S0368-2048(97)00028-5.